

Environmental effect on sclerometric brittleness of ionic crystals

L. A. KOCHANOVA, V. M. KUCHUMOVA, V. I. SAVENKO, E. D. SHCHUKIN
Institute of Physical Chemistry RAN, Leninskii pr. 31, Moscow, 117915, Russia

The conditions of plastic-to-brittle transition during microscratching with a Vickers diamond indenter of natural cleavage surfaces of lithium fluoride (LiF) single crystals (pure samples and those covered with octadecylamine films) in heptane, distilled water, and their saturated aqueous solution, were studied. Indenter loads varied in the range 3.2×10^{-3} – 1.9×10^{-1} N; indent or sliding velocity was $30 \mu\text{m s}^{-1}$. Quantitative characteristics of microplasticity and microbrittleness of near-surface layers in single crystals under appropriate test conditions were studied. The basic mechanisms of crack formation in non-uniform indenter-induced fields of stresses and deformations were revealed and the active media effect on the relative intensity of the functioning of these mechanisms was analysed.

1. Introduction

Studies of the influence of the surface and environment on strength and plasticity of solids reveal a fundamental peculiarity of mechanical properties of materials, i.e. their physico-chemical character [1–5]. Active media atoms taking part in the deformation process play an essential role in the reconstruction and rupture of interatomic bonds and thus predetermine the character of the destruction of products under conditions of fabrication and use. In this respect, the physico-mechanical aspect of studies of the destruction mechanics of materials in contact interactions is of great practical interest. This is particularly true for studies of the transition from plastic to brittle contact, where, depending on the nature of the media, the plasticizing or embrittling effect can be observed even for a very slight physico-chemical influence, which, in turn, allows the simultaneous study of the work of the competing mechanisms of the respective effects in near-surface layers of the solids. In addition, insight into plasticizing and embrittling mechanisms enables any specialist to develop the optimum conditions for the working of numerous production and technological processes, when including contacts affecting an instrument on material as an operational element of these processes. Thus, taking the physicochemical factor into account, a quantitative description of the plastic-to-brittle transition in contact is a vital scientific and technological problem.

This paper presents the results of studies of plastic-to-brittle transition conditions in near-surface layers of ionic crystals under sclerometric tests in polar and non-polar media.

2. Materials and methods

Lithium fluoride single crystals with a macroscopic yield strength of 1.7 GPa were chosen for the study,

because they modelled the behaviour of fabricated ceramic materials and rocks subjected to the effect of physico-chemical factors. The total concentration of two-valent impurities did not exceed 10^{-3} mol %, and the initial density of growth dislocations was 10^4cm^{-2} . Samples were in the form of plates with dimensions $5 \times 5 \times 2 \text{mm}^3$ and were faceted with cleavage planes $\{001\}$.

Sclerometric tests consisted in making a series of microscratches on the sample surface with a Vickers pyramid indenter, i.e. a diamond indenter with the angle between opposite planes at the apex being 136° . In the process of microscratching the pyramid slide, cutting edge first, along the largest side of the sample completely submerged in a medium, in the $\langle 110 \rangle$ direction of its crystal lattice.

Single scratches were made at room temperature using a PMT-3 device with a vibration-protected unit [6] and indenter loads in the range $P = 3.2 \times 10^{-3}$ to 1.9×10^{-1} N. Each microscratch was indented with a constant load at the tangential velocity of indenter sliding motion $v = 30 \mu\text{m s}^{-1}$. The microscratches varied in length from ~ 2 – 3 mm.

Doubly distilled water and LiF saturated aqueous solution (at room temperature) were used as active (polar) media. An aqueous environment was chosen because of its high adsorption activity relative to alkaline halide crystals [7, 8]. Heptane served as an inactive (non-polar) medium.

The experiments were partially carried out on single crystals covered with octadecylamine (ODA) films. Films were deposited on sample surfaces by pouring onto them a quantity of ODA dissolved in heptane (with a solution concentration of $2 \times 10^{-3} \text{mol l}^{-1}$) and by subsequently evaporating the solvent. The thickness of the coating obtained in this manner was ≈ 35 ODA monolayers.

Under these experimental conditions, the sliding of

the indenter along the sample surface was accompanied by the appearance of a plastic groove (microscratch) on its working surface. After etching the sample in ferrous chloride saturated aqueous solution, a zone plastic deformation developed on each side of a groove i.e. an area where the dislocation density was so high that individual dislocation etch pits could not be distinguished optically ("plastic" zone), and a larger zone could also be seen occupied by individually distinguishable dislocations (dislocation "path"). (Etch pit dimensions in these experiments were about 1 μm .)

With increasing indenter loads, above some critical value characterizing each medium, microcracks appeared in the plastic zone and spread from groove borders along the $\langle 110 \rangle$ directions and at an acute angle ($\approx 45^\circ$) to the indenter motion direction (see Fig. 1). As previously, the following characteristics of plastic deformations in contact were used [9, 10]: groove width, $2a$, width of dislocation path, $2L$, surrounding the groove, and plastic zone width, $2l_{pl}$. For characterization of microbrittleness of a material, the width of the brittle zone, $2l_{tr}$, was used which was defined as the redoubted mean length of vertical projections of cracks spread on each side of a groove (see Fig. 1). In addition, the tendency to brittle destruction in a material under indenter loads above a critical value was estimated using the linear crack density. The latter was determined by calculating the quantity of cracks per unit length of indenter track at constant load. The results of each experiment were averaged on the basis of not less than 100 scratches.

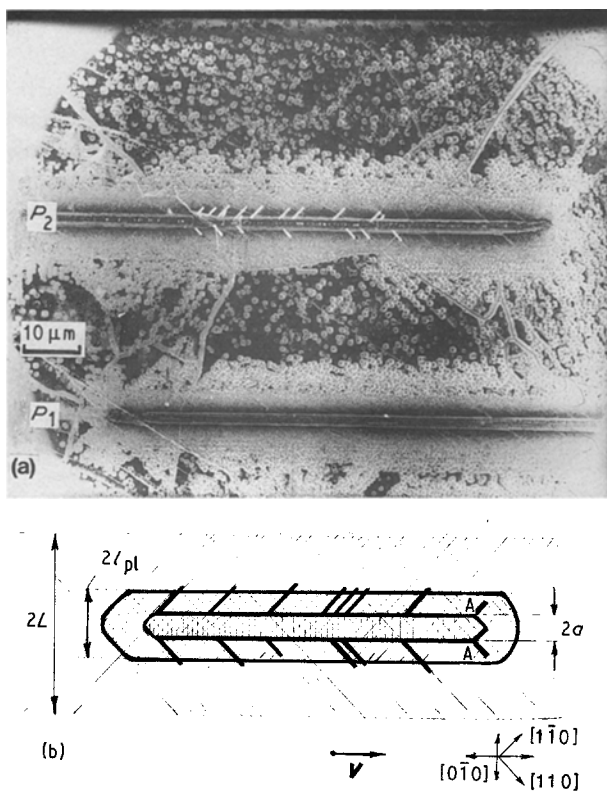


Figure 1 (a) Microphotograph of LiF sample surface after sclerometric tests in heptane and subsequent selective etching; and (b) schematized zone structure of a scratch obtained with $P \geq P_c$, $P_1 = 3.3 \times 10^{-2}$ N, $P_2 = 4.2 \times 10^{-2}$ N. Explanatory notes are given in the text.

3. Results

Figs 2 and 3 show the main plastic characteristics of microscratches versus indenter loads in various media. Graphic-analytical processing of the curves revealed that in many cases they may be described by power functions of the following form

$$2a = A_a \cdot P^{n_a} \quad (1a)$$

$$2L = A_L \cdot P^{n_L} \quad (1b)$$

The experiments show that indices n practically do not change during transition from plastic to brittle contact (see Figs 2, 3 and Table I). Similar relationships have been previously reported [9] for an LiF single crystal – spherical diamond indenter contact pair during scratching of samples in air. The fact that n_a and n_L do not differ much in their numerical values, practically determines the independence of the relation L/a from indenter load and this, in turn, indicates the validity of the law of mechanical similarity of LiF near-surface layer plastic deformation under the experimental conditions.

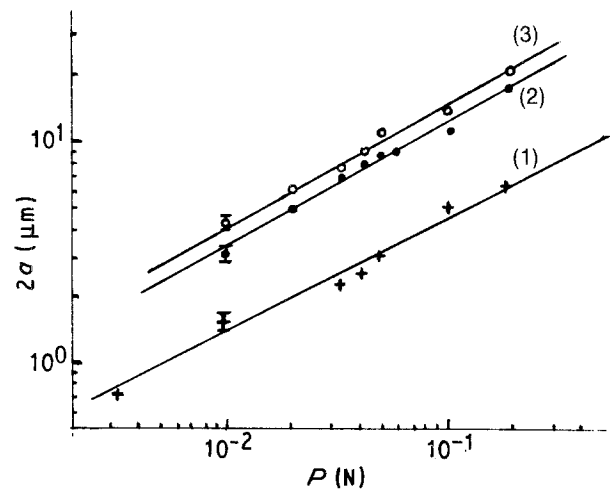


Figure 2 Groove width – indenter load relationship under sclerometric tests of (1) LiF in heptane, (2) LiF in saturated salt solution, and (3) water.

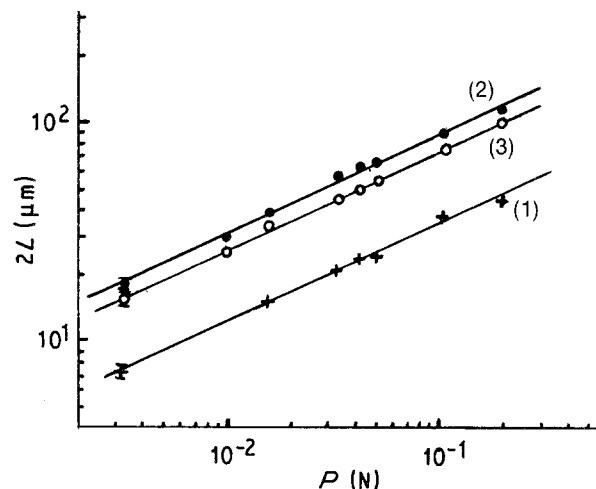


Figure 3 Dislocation path width – indenter load relationship under tests of (1) LiF in heptane, (2) LiF in saturated salt solution, and (3) water.

TABLE I Numerical values of parameters of Equation 1 and critical values of threshold load, P_c , of cracking obtained after scratching samples in various media

| Medium | n_a | n_L | A_a | A_L | P_c , (10^{-2} N) |
|----------------------------|-----------------|-----------------|---------------------------------------|---------------------------------------|------------------------|
| | | | ($\mu\text{m N}^{-1}$) ^a | ($\mu\text{m N}^{-1}$) ^a | |
| Heptane | 0.52 ± 0.01 | 0.46 ± 0.01 | 14.5 ± 0.2 | 100 ± 1.5 | 4.2 ± 0.3 |
| LiF aqueous solution | 0.57 ± 0.01 | 0.47 ± 0.01 | 44.5 ± 0.5 | 260 ± 5 | 3.3 ± 0.2 |
| Water | 0.57 ± 0.01 | 0.46 ± 0.01 | 54.0 ± 1.0 | 215 ± 5 | 1.6 ± 0.4 |
| Water: ODA-covered samples | — | — | — | — | 4.2 ± 0.3 |

The results given in Figs 2 and 3 show a considerable influence of active media on the plastic deformation of a surface in near-contact areas: widths of grooves, dislocation paths and plastic zones in aqueous media prove to be markedly larger in size than in heptane. Aqueous media also exert an essential influence on the characteristics of brittle destruction of a surface. At the same indenter load, brittle zone sizes increase with medium change in the following order: heptane – LiF saturated aqueous solution – water (Fig. 4). However, the most drastic changes, as a result of media changes, are observed in the linear density of cracks which, all other things being equal, determines probability of brittle destruction of a crystal surface layer (Fig. 5). A more active medium causes a substantial increase in velocity of linear crack density growth with increasing load. But ODA films on sample surfaces markedly decrease this phenomenon.

Table I also lists threshold values of loads P_c corresponding to the appearance of the first cracks along the indenter trace. Apparently, it is these loads that determine the transition from plastic to brittle contact in the respective media. As may be seen from the table plastic–brittle transition shifts to lower loads with higher medium activity. P_c grows if the single crystal surface is covered with ODA film which confirms the protective effect of this film. This effect also manifests itself in a decrease of the probability of brittle destruction of the sample in water under critical load.

The elementary half-empirical theory of formation of the “fir-line” lateral cracks during indenter

scratching developed by Veldkamp *et al.* [11] allows us to establish a relationship between contact geometrical and load parameters, on the one hand, and material strength characteristics, on the other. In the designations used in the present work, the above relationship has the following form:

$$\mu P = A_c K_c [l_{fr}^2 (l_{fr} - B_a)]^{1/2} \quad (2)$$

where μ is the indenter–sample friction coefficient, K_c the critical value of the stress intensity factor determining the lateral crack formation, A_c is a constant depending only on indenter geometry and crack form (the latter is assumed to be close to elliptical), B a dimensionless parameter whose numerical value is defined by the location of the crack’s central elliptical section relative to the groove axis.

Using Equation 2 and taking into account that, under these experimental conditions, $\mu = 0.28$ [9] and $A_c = 3.14$ [11], the results given in Figs 2 and 4 allow us to determine the values of K_{lc} for cracks formed in $\{110\}$ -type planes of LiF single crystals in the media used in the experiment. Also assuming that

$$K_{lc}^2 = 2\gamma_{\langle 110 \rangle} E_{\langle 110 \rangle} / (1 - \nu^2) \quad (3)$$

where $E_{\langle 110 \rangle} = 124$ HPa (calculated from [12]), $\nu \approx 1/3$, and $\gamma_{\langle 110 \rangle}$ is the effective energy of crack surface unit formation, it is not difficult to find absolute values of this energy under the above test conditions.

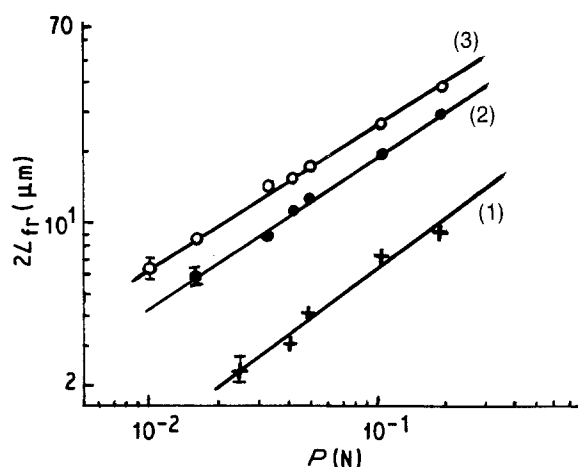


Figure 4 Brittle zone width – indenter load relationship under tests in various media. (1) LiF in heptane, (2) LiF in saturated salt solution, and (3) water.

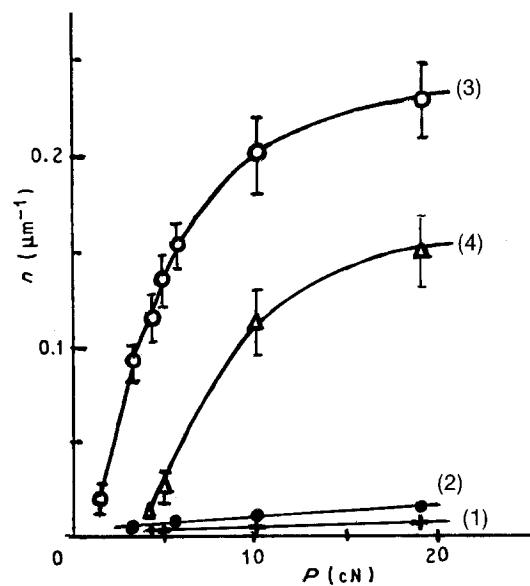


Figure 5 Linear crack density (n) – indenter load (P) relationship for scratches obtained (1) in heptane, (2) in LiF saturated aqueous solution, (3) in water, and (4) in water on ODA-covered samples.

tions. The results of the appropriate calculations are given in Table II.

According to modern ideas (see, for example, [2–5]), crack formation in elastic–brittle and quasi–brittle solids consists of two stages: in the first stage, a relatively slow precritical growth of an embryonic equilibrium microcrack (flaw) can be observed and when it attains critical values, the second stage, speedy crack spread in the outer stress field, occurs. The theoretical relationships [11] are good in describing mainly the final stage of crack formation during indenter scratching and do not allow estimation of critical dimensions of those embryonal submicrocracks where lateral cracks actually develop. A theory making this possible in terms of linear mechanics of destruction, i.e. a theory describing crack formation in the process of indenter scratching of absolutely elastic–brittle materials, has been developed previously [13]. Similar methods can also be used (with appropriate changes) for the estimation of critical dimensions of embryonic submicrocracks responsible for the transition to the second stage of crack formation in plastic–brittle contact in ionic crystals. The use of the destructive linear mechanics approach in the present case can be substantiated by the following experimental observations.

1. Despite the fact that the material is in a plastic state in the near-surface area, growth of lateral cracks during indentation takes place in the form of cleavage brittle destruction in one crystallographic plane of $\{110\}$ type.

2. With growth of a crack, additional plastic deformation of the surrounding material occurs only in a narrow near-surface layer at the edge of the crack.

These peculiarities of crack spread in sclerometric tests of ionic crystals allow us to assume that unloading of the material near crack borders during crack propagation occurs in accordance with a law similar to the linear-elastic one. Then, still taking Griffiths' brittle destruction criterion as a basis and following the method proposed previously [13], it would be of no difficulty to show that the condition determining the dimensions of an equilibrium lateral crack, $C_{cr} = (l_{tr} - a)_{cr}/\cos 45^\circ$, and the critical length of its submicroembryo, C_f , alike, has the form

$$\pi(1 - \nu^2)\{K_I^2 + K_{II}^2\} \geq 2\gamma_{\langle 110 \rangle} E_{\langle 110 \rangle} \quad (4a)$$

$$K_I = \frac{2}{\pi}(c)^{1/2} \int_0^{c/a} \frac{\sigma_n(x) dx}{[(c/a)^2 - x^2]^{1/2}} \quad (4b)$$

$$K_{II} = \frac{2}{\pi}(c)^{1/2} \int_0^{c/a} \frac{\tau(x) dx}{[(c/a)^2 - x^2]^{1/2}} \quad (4c)$$

TABLE II Medium effect on characteristics of cracking in $\{110\}$ planes after scratching of LiF single crystals

| | Heptane | LiF aqueous solution | Water |
|-------------------------------|---------------|----------------------|-----------------|
| B | -6 ± 1 | $+1.6 \pm 0.1$ | $+6.6 \pm 0.4$ |
| $K_{Ic} (\text{MN m}^{-3/2})$ | 0.7 ± 0.1 | 0.41 ± 0.02 | 0.38 ± 0.02 |
| $\gamma (\text{J m}^{-2})$ | 1.9 ± 0.6 | 0.61 ± 0.06 | 0.53 ± 0.05 |

where c is the current crack length; $x = r/a$; r is the distance along this length. In the above relationship, the normal $\sigma_n(x)$ and tangent to the crack plane $\tau(x)$ components of the tensor of stresses induced by the indenter and causing crack growth, may be calculated on the basis of previous results [4]. It would be only natural to think that transition to the second stage of crack formation under threshold load must occur primarily in those contact area spots where the density of elastic energy, which is realising from the material during crack growth attains its maximum value. Calculations show that, in the case of “fir” cracks lying in type $\{110\}$ planes and spreading in $\langle 110 \rangle$ directions, this condition takes place near the points of the plastic groove surface where the groove breaks away from the indenter frontal section (AA in Fig. 1). In these points, tensor components σ_n and τ Equation 4a–c attain their maximum values at the same time and their change in points along the way from groove borders in the $\langle 110 \rangle$ directions can be described, as a first approximation, by functions of the following form:

$$\sigma_n(x) = \frac{2Y}{3^{1/2}} \ln \left(\frac{l_{pl}/a}{1 + x \cos 45^\circ} \right) \quad (5a)$$

$$\begin{aligned} \tau(x) &= \tau_s \\ &= \frac{Y}{3^{1/2}} \end{aligned} \quad (5b)$$

when $x \leq (l_{pl} - a)/a \cos 45^\circ$,

$$\sigma_n(x) = 0 \quad (6a)$$

$$\tau(x) = \frac{Y}{3^{1/2}} \left(\frac{l_{pl}/a}{1 + x \cos 45^\circ} \right)^2 \quad (6b)$$

when $x > (l_{pl} - a)/a \cos 45^\circ$.

where Y is tensile yield strength of hardened material. By analogy with [14], $Y/3^{1/2}$ should be taken as equal to $H/[1 + 2 \ln(l_{pl}/a)]$, where $H = \kappa P/\pi a^2$. Static-sliding contact transition in expressions (5) and (6) takes place when $\kappa = 2$ and it is taken into account by changing values of the characteristic l_{pl} accordingly. Taking into consideration the experimental relation $l_{pl} \approx l_{tr}$ and using data given in Figs 2 and 3, it can be shown that, in the present experiment, the relationship $K_I < K_{II}$ is true for $\{110\}\langle 110 \rangle$ fir cracks in sliding contact. In the other words, microcracks lying, for example, in $\langle 110 \rangle$ planes spread in $[110]$ directions during the second stage of their growth, mainly under the effect of tangent stresses which, in terms of the given approximation, are constant in the developed plastic deformation zone and sharply decrease beyond the latter. Then, taking into account that $l_{tr} = a + c \cos 45^\circ$ and $c_f/a \ll 1$, Equations 4a–c may be suitably transformed to evaluate the critical dimensions of embryonic submicrocracks determining transition to the second stage of their growth

$$c_f = \frac{\pi a^4 \gamma_{\langle 110 \rangle} E_{\langle 110 \rangle} [1 + 2 \ln(l_{pl}/a)]^2}{(1 - \nu^2) 2P^2 [1 + 4 \ln^2(l_{pl}/a)]} \quad (7)$$

c_f values calculated from Equation 7 for threshold loads P_c , on the basis of experimental data (see Figs 2, 3), with the values of $\gamma_{\langle 110 \rangle}$ defined above being taken into consideration, are listed in Table III. The results

TABLE III Values of cracking and microplasticity characteristics of LiF single crystals scratched in various media at threshold loads

| | Heptane | LiF aqueous solution | Water | Water ODA-covered samples |
|--|-----------------|----------------------|-----------------|---------------------------|
| $P_c (10^{-2} \text{ N})$ | 4.2 ± 0.3 | 3.3 ± 0.2 | 1.6 ± 0.4 | 4.2 ± 0.3 |
| $c_{cr} (\mu\text{m})$ | 0.35 ± 0.04 | 1.96 ± 0.2 | 2.87 ± 0.2 | – |
| $c_f (10^{-2} \mu\text{m})$ | 0.15 ± 0.05 | 2.4 ± 0.3 | 4.1 ± 0.4 | – |
| $c_d^{\text{max}} (10^{-2} \mu\text{m})$ | 0.6 ± 0.2 | 12 ± 2 | 26 ± 3 | – |
| $\tau_s^a (\text{GPa})$ | 9.8 ± 0.5 | 1.2 ± 0.05 | 0.76 ± 0.04 | – |

^a Yield strength value of material in deformation-hardened near-contact zone.

of these calculations, as well as data given in Fig. 5, point to the fact that embryonic submicrocracks of considerable dimensions and in rather high concentrations should exist in samples to cause transition to the second stage of crack formation under the conditions described. But biographic submicrocracks with similar characteristics were not observed in the artificial almost perfect single crystals used in this work. Therefore, it is natural to think that such submicrocracks arise during the process of indentation and originate because of dislocations. They appear in the plastic deformation zone due to stress concentrators which are the stopped dislocation rows in a slip bands; the dislocations have lost their mobility as a result of dislocation reactions in crossing slip planes [15]. It is helpful to compare dimensions of dislocation microcracks, c_d , arising in this way at threshold indenter loads, with those of critical embryonic submicrocracks, c_f . c_d may be evaluated in terms of various models of dislocation crack formation in conditions of inhomogeneous crystal plastic deformation [16, 17]. Most models give values of equilibrium microcrack dimensions similar in order.

A generalized model of dislocation microcrack formation through opening of the stopped part of a slip band [18, 19] was considered as an example most adequately approximating to reality. In this case, the equation system defining the maximal possible value of c_d^{max} has the form

$$\left. \begin{aligned}
 c_d^{\text{max}} 8\pi(1-\nu)\gamma &= (nb)^2 G; \\
 Gnb &= \pi(1-\nu)\tau_{ef} \delta \\
 2\gamma G &= \tau_{ef}^2 \pi(1-\nu)\delta; \\
 \tau_{ef} &= \tau_s - \tau_0; \tau_0 = 2Gnb/\delta \\
 G &= E/2(1+\nu); \tau_s = Y/3^{1/2},
 \end{aligned} \right\} (8)$$

where b is the modulus of dislocation Burgers vector, G the shear modulus, δ the length of the stopped part of the slip band ($c \ll \delta$), and τ_0 the initial stress of the operating of dislocation sources.

The results of calculations of c_d^{max} for threshold loads are listed in Table III. Comparison of c_f and c_d^{max} shows that, in all cases considered, the preliminary plastic deformation in the near-contact zone is quite sufficient to cause the occurrence of embryonic submicrocracks of proper dimensions in this area.

4. Discussion

Benson [20] gives the value $\gamma_{\{110\}} = 568 \text{ mJ m}^{-2}$ of surface energy at LiF $\{110\}$ surface in local coordin-

ate approximation on the basis of interatomic forces calculations in ionic crystals. The experiments of Gilman [21] show the correctness of this estimation. Proceeding from it, a critical value of the stress intensity factor necessary for propagation of an absolutely brittle crack lying in the $\{110\}$ plane may be calculated from Equation 3: $K_{Ic}^{\{110\}} = 0.39 \text{ MN m}^{-3/2}$. Comparison of the published theoretical value with experimental data leads to the conclusion that the predominant part of the energy in the process of "fir" crack formation during scratching is spent on the work aimed at an additional plastic deformation of the material near the crack tip.

The results given in Figs 2–5 and in Tables I–III, make it possible to affirm, that in tests under consideration, aqueous medium exerts both plasticizing and embrittling influence on lithium fluoride. The plastic by the effect is manifested by an increase in all zone dimensions characterizing plastic deformation around the scratch, decrease of nominal contact pressure $2P/\pi a^2$, and, as a consequence, by growth of the critical dimensions of embryonic submicrocracks, c_f , during transition from heptane to aqueous media. The embrittling effect of the latter is attested by decrease in the P_c level, growth of linear crack density and increase in their final dimensions determining the width of the brittle zone. At the same time, the relative intensity of the manifestation of plasticizing and embrittling effects in the experiments under consideration, differs substantially. In fact, analysis of the experimental data obtained by Yu Yao [22] shows that water adsorption in thermodynamic equilibrium conditions lowers the surface energy in LiF by only 30%. In our case, a decrease in the effective surface energy, γ , under an aqueous medium effect in the conditions of crack formation, is about 70% (see Table II). Simple calculations based on these data reveal that in our experiments, an aqueous medium lowers by almost 90% that part of γ connected with plastic deformation which accompanies opening of a crack. This result, together with the decrease in crack formation threshold under tests in an aqueous medium, means that the embrittling effect of the latter is predominant under fairly high indenter loads, $P > P_c$. On the other hand, experience shows that, during transition from LiF saturated aqueous solution to an unsaturated one (formed initially in distilled water) under fairly low indenter loads $P \lesssim P_c$, a medium plasticizing effect proves to be much more evident than an embrittling one. These experiments clearly reveal that it is possible, in principle, to control

the comparative intensities of different forms of medium effects on the mechanical state of a material by varying the degree of medium activity, outer force value and, possibly, velocity of scratching.

The results obtained also show that plastic-to-brittle transition during scratching is inevitably related to the occurrence of local plastic deformation heterogeneities and, as a result, to abrupt local stress concentrations. In order that an embrittling medium effect could be manifested, even at a marked decrease of surface energy, a material should have structural defects, in this case, dislocation and stopping obstacles, because it is the dislocation-obstacle interactions that bring about deformation heterogeneities in sliding bands, thus causing a stress concentration around the former. In this way, conditions are produced for embryonic submicrocrack formation and their subsequent growth to equilibrium dimensions.

The presence of the active medium on the crystal surface, on the one hand, results in a decrease of yield strength, τ_s , (see Table III), of the hardening coefficient of a material in contact [23] and, as a result, contributes to general lowering of stresses active in the near-surface area. On the other hand, due to the decrease in effective surface energy, critical values of tangential (and normal) components of the stress tensor determining the formation of submicrocracks near the stress concentrators, considerably diminish. Thus, competition between plasticizing and embrittling mechanisms can be clearly observed under the effect of surface-active media. The more pronounced intensity of one of the mechanisms, under the given test conditions, is what finally determines the shift in the direction of the plastic-to-brittle transition threshold of the material.

It was previously shown [24] that when holding ionic crystals in contact with phase volumes of surfactants in aqueous solutions, water may prove to have not only an adsorption but also a solvent effect on the crystals. But regression analysis of the data in Fig. 4 shows that relationships $l_{fr} = f(P)$ obtained in active media and in heptane have a common pole at the beginning of the coordinates. This allows us to draw the conclusion that a process of dissolving of crystal surface layers in water is weakly pronounced even in such surface locations with considerable energetic heterogeneity as the crack borders are. The latter fact is conditioned by a rather low solubility of LiF in water (1.2 g l^{-1} at room temperature). Thus, it would be reasonable to assume that the influence of aqueous media on the characteristics of LiF surface "destructability" under sclerometric testing is mainly related to the Rehbinder effect [1].

At the same time, microscopic observations of the surface of samples held for prolonged periods of time (several hours) in active media confirm that local selective dissolving of material at lattice defects still takes place. In distilled water it is more evident than in aqueous saturated salt solution. Because in the case of distilled water, the dissolving is more active in removing surface layer hardening [25], it substantially reduces the portion of the effective surface energy, γ , caused by plastic deformation, and markedly intensi-

fies the plastic deformation processes in the slip bands belonging to different crystallographic systems. As a result, in the transition from saturated salt solution to water, the formation process of dislocation submicrocracks and their further development to equilibrium cracks with larger final dimensions, are greatly facilitated and take place at a much lower level of outer forces (see Table III). In this way the radical shift of threshold crack formation load towards lower values can be explained, as well as the increase in brittle zone width in samples tested in distilled water, compared to those tested in LiF saturated aqueous solution. (It should be noted that water adsorption on crack surfaces slows down healing of the latter after unloading [26].)

A slight reduction of dislocation zone dimensions around scratches observed in transition from tests in aqueous saturated salt solution to those in distilled water is related to the more intensive etching of points of dislocation emergence on the crystals free surface. The resulting decrease in mobility of dislocations which are leading in the slip bands (their "blocking" [27]) should be the main cause of the observed effect.

Within the limits of the previously studied models, a consistent explanation can be offered for the linear crack density-load, P , relationship and for its change under active media influence.

When considering the data presented in other works [24, 28], it can be assumed that the protective effect of ODA film results from the hydrophobicity of the sample surface caused by ODA molecules which prevent direct contact of the sample with water, thus creating a shielding effect. The effectiveness of the shielding is determined, in this case, by the strength of the adsorption bond of ODA molecule amine groups to the LiF sample surface and by the cohesion strength of ODA hydrocarbonic chains [29].

5. Conclusions

1. Quantitative characteristics of microplastic deformation and crack formation during microscratching of LiF single crystals in inert and active media were determined.
2. The basic mechanisms of crack formation under sclerometric tests of elastic-brittle materials with limited plasticity were analysed in terms of destructive linear mechanics.
3. It was shown that dealing with varying damaging conditions, the nature and degree of activity of the environment, as well as contact deformation velocities, it is possible to control efficiently the intensity of plasticizing and embrittling effects on materials during the course of the processing.

References

1. V. I. LIKHTMAN, E. D. SHCHUKIN and P. A. REHBINDER, "Physico-Chemical Mechanics of Metals" (AN SSSR, Moscow, 1962).
2. R. M. LATANISION and J. T. FOURIE (eds), "Surface Effects in Crystal Plasticity" (Noordhoff, Leiden, 1977) p. 944.
3. J. M. GEORGES (ed.), "Microscopic Aspects of Adhesion and Lubrication" (Elsevier, Amsterdam, 1982).

4. P. LACOMBE (ed.), "Physical Chemistry of the Solid State: Application to Metals and their Compounds" (Elsevier, Amsterdam, 1984).
5. E. D. SHCHUKIN, V. I. SAVENKO and L. A. KOCHANOVA, *Poverkhnost* **7** (1985) 106.
6. G. P. UPIT and S. A. VARCHENYA, in "Novoye v oblasti ispytaniy na mikrotverdst" (Nauka, Moscow, 1974) p. 128.
7. E. D. SHCHUKIN, N. V. PERTSOV and R. I. ZLOCHEVSKAYA (eds), "Physico-Chemical Mechanics of Natural Disperse Systems", edited by M. M. Hrushchov (Moscow State University, Moscow, 1985).
8. V. I. SAVENKO, L. A. KOCHANOVA and E. D. SHCHUKIN, *Treniye i iznos* **5** (1984) 43.
9. V. I. SAVENKO, V. N. LVOV, L. A. KOCHANOVA and E. D. SHCHUKIN, *Fiz. i Khim. Obrab. Mater.* **1** (1978) 131.
10. N. P. FEDOSEEVA, L. A. KOCHANOVA, V. I. SAVENKO and E. D. SHCHUKIN, *ibid.* **6** (1983) 86.
11. J. D. B. VELDKAMP, N. HATTU and V. A. C. SNIJDERS, in "Fracture Mechanics of Ceramics" edited by R. C. Bradt, D. P. H. Hasselman and F. F. Lange, Vol. 3 (Plenum Press, New York, London, 1978) p. 273.
12. H. B. HUNTINGTON, *Solid State Phys.* **7** (1958) 213.
13. B. R. LAWN, *Proc. R. Soc. Ser. A* **299** (1967) 307.
14. C. M. PERROT, *Wear* **45** (1977) 293.
15. J. T. HAGAN, *J. Mater. Sci.* **14** (1979) 2975.
16. V. M. FINKEL, "Destruction Mechanics" (Metallurgiya, Moscow, 1970) p. 376.
17. T. YOKOBORI, "An Interdisciplinary Approach to Fracture and Strength of Solids" (Wolters-Noordhoff, Groningen, 1968) p. 264.
18. R. BULLOGH, *Phil. Mag.* **9** (1964) 917.
19. E. SMITH and J. T. BARNBY, *Metal. Sci. J.* **1** (1967) 56.
20. G. S. BENSON, *J. Chem-Phys.* **35** (1961) 2113.
21. G. G. GILMAN, *J. Appl. Phys.* **31** (1960) 2208.
22. Y. F. YU YAO, *J. Coll. Sci.* **28** (1968) 376.
23. A. E. SMIRNOV, A. A. URUSOVSKAYA and V. R. REGEL, *DAN SSSR* **280** (1985) 1122.
24. N. I. IVANOVA, N. G. VAKAR and N. V. PERTSOV, *J. Prikl. Khim.* **60** (1967) 1504.
25. L. E. REZNIK and A. A. SHPUNT, *Kristallogr.* **19** (1974) 1118.
26. D. H. ROACH, D. M. HEUCKERETH and B. R. LAWN, *J. Coll. Interface Sci.* **114** (1986) 292.
27. A. R. C. WESTWOOD, J. S. AHERN and J. J. MILLS, *J. Coll. Surf.* **2** (1981) 1.
28. N. I. IVANOVA, N. G. VAKAR and N. V. PERTSOV, *Koll. J.* **49** (1987) 148.
29. A. V. LOBANOV, L. A. KOCHANOVA, V. I. SAVENKO and E. D. SHCHUKIN, *Treniye i iznos* **6** (1985) 790.

*Received 21 June
and accepted 23 July 1991*